JOURNAL OF COMPUTATIONAL PHYSICS 122, 143–149 (1995)

A Weakly Singular Formulation of Boundary Integral Equations and Field Computation near Boundaries

NORIO NAKAGAWA[1]

Center for Nondestructive Evaluation, Iowa State University, Ames, Iowa 50011

Received June 9, 1994; revised October 24, 1994

Applications of the boundary integral equation method to real-world problems often require that field values should be obtained near boundary surfaces. A numerical difficulty is known to arise in this situation if one attempts to evaluate near-boundary fields via the conventional Green's formula. The present work addresses this particular issue. Namely, a stable computational scheme for both fields and gradients in the near-boundary region has been formulated. This approach starts with the conventional Green and Maue representations of fields and gradients written inside and outside of the defining volume. Then, a new set of integral representations that have weaker kernel singularities is derived by canceling the most singular terms between the conventional formulas of the two sides. The principal contribution of this work is the explicit construction of the improved representations for the fields and gradients. Also presented are several numerical results that demonstrate the superiority of the new representations over the conventional ones.

1. INTRODUCTION

It has been recognized that the boundary element method (BEM) has a significant potential to become a prominent numerical technique to solve real-world physical problems. To ensure broader acceptance, many efforts have been directed toward reducing technical complications that arise when dealing with the strong kernel singularity of the basic boundary integral equation (BIE). One successful example can be found in the well-known weak formulation of the BEM that basically eliminates the strong singularity from the solution process. Yet, progress needs to be made in another problem that arises also from the strong kernel singularity. Namely, the conventional Green's formula is known to yield unstable results when the field is evaluated in the vicinity of the boundary. Recently, a method by cancellation was proposed to address this problem [3], and this paper presents a detailed account of the method and its generalization to field derivatives.

The BEM has its foundation in the celebrated formula of Green [1]. However, the aforementioned near-boundary instability originates in Green's formula itself, particularly in its strong kernal singularity that causes rapid changes across the boundary. (See Ref. [3] or Section 2 below for details.) This observation prompted a search for an alternative field representation that replaces Green's formula, while expressing fields continuously near the surface. It was demonstrated [3] that such an improved formula is attainable when the known arbitrariness of Green's formula [4–6] is exploited. There, it was also mentioned briefly that the same procedure applies to Maue's gradient representation [2], resulting in weaker kernel singularities. In Section 3 below, the derivations of these improved formulas are given explicitly. We will show subsequently in Section 4 that the improved formulas in fact yield stable results when applied to the near-boundary field calculation. These formulas are more suitable for practical applications than the conventional ones because they require no sophisticated element integration algorithms, thus simplifying software implementation.

The subsequent sections are organized as follows. Section 2 formulates the near-boundary singularity problem explicitly. Both field and gradient representations are examined in a parallel fashion, starting with Green's and Maue's formulas. In passing, both the formulas are turned into weakly singular BIEs. Most of the materials in Section 2 are of standard nature, except that the weakly singular BIE (2.15) derived from the Maue representation is less conventional. Next, our improved field and gradient representations are derived in Section 3. The method is based on cancellation between formulas written inside and outside the defining region, and formulated in single-phase problems. The numerical test results are presented in Section 4 to demonstrate the validity of our approach. In Section 5, the relationship between the single-phase and multiple-phase problems is pointed out. Finally, Section 6 contains concluding remarks.

2. STATEMENT OF THE NEAR-BOUNDARY INSTABILITY PROBLEM

As a preliminary, we will formulate near-boundary field evaluation based on the conventional Green and Maue formulas, in order to identify the origin of numerical instabilities. To be explicit, let us consider a scalar Helmholtz problem. Let φ be

[1] E-mail: nnakagaw@cnde.iastate.edu.

0021-9991/95 $12.00

a scalar field in a finite volume V that satisfies the equation

$$[\nabla^2 + k^2]\varphi = -J, \tag{2.1}$$

where J is a source. Also let S be the boundary surface of V, $\vec{n}$ be the outward-directed surface normal vector, and u and v denote the field and its normal derivative, i.e.,

$$\varphi \equiv u, \quad \nabla_n \varphi \equiv v, \tag{2.2}$$

on S. Then, the field and its gradient inside V can be expressed in terms of u and v via Green's and Maue's formulas,

$$\chi_P \varphi_P = \varphi_P^{(0)} + \int_S dS[(-\nabla_n G)u + Gv], \tag{2.3}$$

$$\chi_P(\vec{\nabla}\varphi)_P = (\vec{\nabla}\varphi^{(0)})_P + \int_S dS[(\vec{\nabla}G) \times (\vec{n} \times \vec{\nabla}u) - k^2 \vec{n} G u + (-\vec{\nabla}G)v], \tag{2.4}$$

respectively, where G is the Green's function, $\varphi^{(0)}$ is the source term, and χ is the characteristic function of the volume V. Explicitly,

$$G = G(\vec{x}_P - \vec{x}) = \exp(ikr)/4\pi r, \quad r \equiv |\vec{x}_P - \vec{x}|, \tag{2.5}$$

$$\varphi_P^{(0)} = \int_V dV\, GJ, \tag{2.6}$$

and

$$\chi_P = \begin{Bmatrix} 1 \\ 0 \end{Bmatrix} \quad \text{when } P \in \begin{Bmatrix} V \\ \overline{V} \end{Bmatrix}, \tag{2.7}$$

where $\overline{V}$ is the outside region of V. The explicit inclusion of χ in Eqs. (2.3, 2.4) emphasizes that the representations are valid and give vanishing results outside V. It should be remarked that Eq. (2.4) is related to the direct derivative of (2.3),

$$\chi_P(\vec{\nabla}\varphi)_P + (\vec{\nabla}\chi)_P \varphi_P = (\vec{\nabla}\varphi^{(0)})_P + \int_S dS[(\nabla_n \vec{\nabla}G)u + (-\vec{\nabla}G)v], \tag{2.8}$$

through Stokes' theorem.

Two important special cases should be noted here: One is a constant field φ, $\varphi = 1$, in V. Since $\nabla^2\varphi = 0$, Eq. (2.3) applies to this field, resulting in a representation of χ,

$$\chi_P = \int_S dS(-\nabla_n G_0), \quad G_0 \equiv 1/4\pi r. \tag{2.9}$$

Second, consider a field φ defined by the relation $\varphi = \vec{a} \cdot \vec{x}$ where $\vec{a}$ is a given constant vector. Since $\nabla^2\varphi = 0$ also while $\vec{\nabla}\varphi = \vec{a}$, Eq. (2.4) can be used to give another χ representation

$$\chi_P \vec{a} = \int_S dS[(\vec{\nabla}G_0) \times (\vec{n} \times \vec{a}) + (-\vec{\nabla}G_0)(\vec{n} \cdot \vec{a})]. \tag{2.10}$$

The well-known weak formulation can be obtained from Eqs. (2.3) and (2.9): Let Q be a point of S, and u_Q be the value of u at Q. Then, by subtracting Eq. (2.9) times u_Q from (2.3), one finds that

$$\chi_P(\varphi_P - u_Q) = \varphi_P^{(0)} + \int_S dS[\{-\nabla_n(G - G_0)\}u - (-\nabla_n G_0)(u - u_Q) + Gv]. \tag{2.11}$$

Also, a similar (but less frequently used) procedure is applicable to Eqs. (2.4) and (2.10): Letting

$$\vec{a} \equiv (\vec{\nabla}\varphi)_Q = (\vec{\nabla}_t u)_Q + \vec{n}_Q v_Q \tag{2.12}$$

in Eq. (2.10), and subtracting it from (2.4), we find that

$$\begin{aligned}\chi_P\{(\vec{\nabla}\varphi)_P - (\vec{\nabla}\varphi)_Q\} = {} & \vec{\nabla}\varphi_P^{(0)} + \int_S dS[\{\vec{\nabla}(G - G_0)\} \times (\vec{n} \times \vec{\nabla}u) \\ & - k^2 \vec{n} G u + \{-\vec{\nabla}(G - G_0)\}v] \\ & + \int_S dS[(\vec{\nabla}G_0) \times \{\vec{n} \times (\vec{\nabla}u - \vec{\nabla}\varphi_Q)\} \\ & + (-\vec{\nabla}G_0)\{v - \vec{n} \cdot \vec{\nabla}\varphi_Q\}].\end{aligned} \tag{2.13}$$

Setting $P = Q$ in Eqs. (2.11, 2.13), and taking the inner product of (2.13) with $\vec{n}_P$, we obtain the weakly singular BIEs

$$0 = u_P^{(0)} + \int_S dS[\{-\nabla_n(G - G_0)\}u - (-\nabla_n G_0)(u - u_P) + Gv], \tag{2.14}$$

$$\begin{aligned}0 = {} & v_P^{(0)} + \vec{n}_P \cdot \int_S dS[\{\vec{\nabla}(G - G_0)\} \times (\vec{n} \times \vec{\nabla}u) \\ & - k^2 \vec{n} G u + \{-\vec{\nabla}(G - G_0)\}v] \\ & + \vec{n}_P \cdot \int_S dS[(\vec{\nabla}G_0) \times \{\vec{n} \times (\vec{\nabla}u - \vec{\nabla}\varphi_P)\} \\ & + (-\vec{\nabla}G_0)\{v - \vec{n} \cdot \vec{\nabla}\varphi_P\}],\end{aligned} \tag{2.15}$$

which can be discretized straightforwardly by the conventional shape-function technique. Among these two, Eq. (2.14) is well-known, and relieves us from explicit Cauchy principal value (CPV) evaluation. It is also known that there is a freedom of choice between the BIEs (2.14, 15) in solving the unknowns, which is useful to avoid fictitious frequency problems, when necessary, by selecting the nondegenerate alternative. What is unique here is that both of the BIEs, particularly Eq. (2.15), are weakly singular.

Given an appropriate boundary condition on S, the unknown

functions u and v can be determined by the BEM from either Eq. (2.14) or (2.15). Let us assume that u and v have been thus determined with sufficient accuracy. In principle, it should be possible to obtain the field and its derivative everywhere in V by evaluating Eqs. (2.3, 2.4). In reality, however, this naive method often fails in the vicinity of S with unstable numerical results. (See Section 4 for some examples.) The origin of this instability is the step-function behavior across S, exhibited explicitly in the representations (2.3, 2.4). Such a rapid behavior is difficult for naive numerical methods to manage. Various numerical techniques have been attempted to remedy the problem. Many of the existing methods require accurate element integration near the collocation point P. Often, the accuracy requirement is so severe that the methods become impractical to apply.

Before proceeding to the next section, we note that it is conceivable to use Eqs. (2.11, 2.13) for near-surface calculation without taking the limit $P \to Q$. Particularly, the idea of using (2.10) to derive (2.13) is useful, and in fact inherited by the method formulated in Section 3, where Eq. (2.10) plays another important role. We will show, however, that our formulas derived in Section 3 are less complicated, and hence easier to implement into computer codes than Eqs. (2.11, 2.13).

3. IMPROVED FORMULAS FOR SINGLE-PHASE PROBLEMS

This section covers our main results, namely, improved representation of fields and derivatives. Given the φ problem in V defined by Eqs. (2.1, 2.2), let us introduce a complementary scalar field ψ that satisfies the equation

$$[\nabla^2 + k^2]\psi = 0, \tag{3.1}$$

in the outside region $\bar{V}$. We also *impose* a boundary condition on ψ so that

$$\psi = u \tag{3.2}$$

on S. Green's and Maue's formulas hold parallel to Eqs. (2.3, 2.4), i.e.,

$$(1 - \chi_P)\psi_P = -\int_S dS[(-\nabla_n G)u + Gw], \tag{3.3}$$

$$(1 - \chi_P)(\vec{\nabla}\psi)_P = -\int_S dS[(\vec{\nabla}G) \times (\vec{n} \times \vec{\nabla}u) - k^2 \vec{n} G u + (-\vec{\nabla}G)w], \tag{3.4}$$

where

$$\nabla_n \psi \equiv w \tag{3.2'}$$

on S. As before, the standard BEM can determine w accurately after casting either (3.3) or (3.4) into a BIE. By adding Eq. (3.3) to (2.3) and Eq. (3.4) to (2.4), we find the improved representations

$$\chi_P \varphi_P + (1 - \chi_P)\psi_P = \varphi_P^{(0)} + \int_S dS\, G(v - w), \tag{3.5}$$

$$\chi_P(\vec{\nabla}\varphi)_P + (1 - \chi_P)(\vec{\nabla}\psi)_P = (\vec{\nabla}\varphi^{(0)})_P + \int_S dS(-\vec{\nabla}G)(v - w), \tag{3.6}$$

for the fields and the derivatives, respectively.

Notice that Eqs. (3.5, 3.6) behave smoother than the usual representations (2.3, 2.4) in the vicinity of the boundary S. For instance, the representation (3.5) is continuous across S. Similarly, Eq. (3.6) represents the tangential derivatives $\vec{\nabla}_t \varphi$ continuously. Discontinuity appears only in the normal component, and it amounts to $\vec{n}_Q(v - w)_Q$ when crossing S through a point Q, where $\vec{n}_Q$ is the surface normal at Q. Therefore, the numerical task has been reduced significantly to dealing with this remaining discontinuity. Here, we use the same technique as in deriving Eq. (2.13). Explicitly, setting $\vec{a}$ equal to the jump $\vec{n}_Q(v - w)_Q$ in Eq. (2.10), and combining it with (3.6), we finally derive the representation

$$\begin{aligned}
&\chi_P(\vec{\nabla}\varphi)_P + (1 - \chi_P)\{(\vec{\nabla}\psi)_P + \vec{n}_Q(v - w)_Q\} \\
&\quad = (\vec{\nabla}\varphi^{(0)})_P + \vec{n}_Q(v - w)_Q + \int_S dS[(-\vec{\nabla}G)(v - w) \\
&\qquad - (-\vec{\nabla}G_0)(v - w)_Q] \\
&\qquad + (v - w)_Q \int_S dS[(-\vec{\nabla}G_0)(1 - \vec{n} \cdot \vec{n}_Q) \\
&\qquad + (-\vec{\nabla}G_0) \times (\vec{n} \times \vec{n}_Q)]
\end{aligned} \tag{3.7}$$

that is fully continuous across the point Q. To ensure the best numerical result, the surface point Q should be chosen sufficiently close to P.

It is Eqs. (3.5, 3.7) that form the foundation of our method. They replace the conventional formulas (2.3, 2.4), and provide a computationally stable method to evaluate φ and $\vec{\nabla}\varphi$ in the volume V, particularly in the vicinity of the surface S. The numerical stability is the immediate consequence of their continuity across the boundary, in sharp contrast with Eqs. (2.3, 2.4).

A few remarks should be made before concluding this section. As was discussed earlier [3], the proposed method requires to solve the BIEs twice. This does not cause a serious computational problem, however. First, Eqs. (2.3, 3.3), for instance, yield a pair of matrix equations of the form

$$\mathbf{A}[u] + \mathbf{B}[v] = -[\varphi^{(0)}], \tag{3.8}$$

$$(\mathbf{1} + \mathbf{A})[u] + \mathbf{B}[w] = 0, \tag{3.9}$$

that share coefficient matrices. Hence, the extra task can be made minimal by avoiding repetitions. Second, the kind of

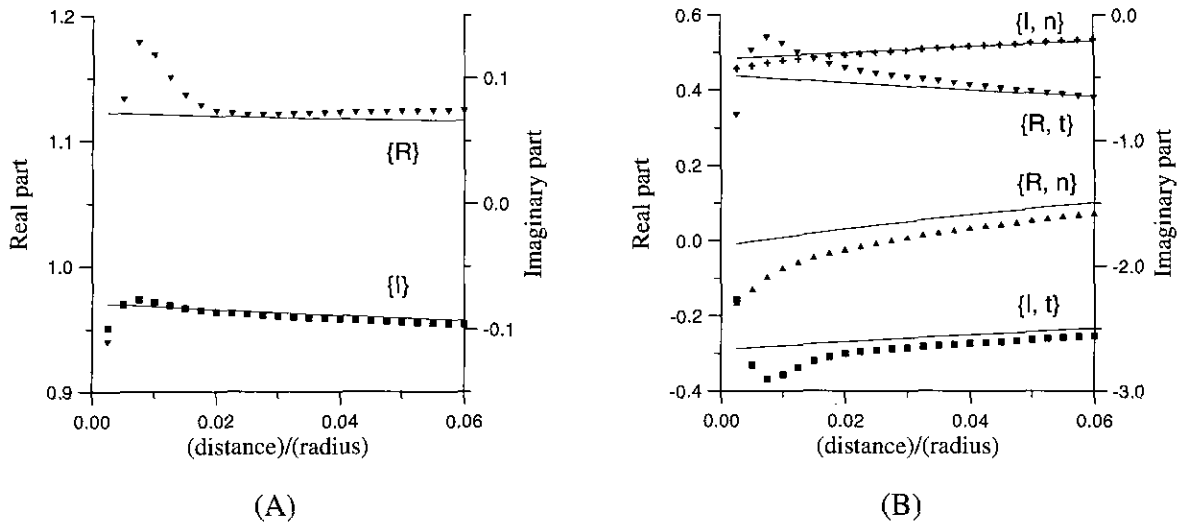

FIG. 1. Plots showing the results of the conventional method via Eqs. (2.3, 2.4). Both the field φ and its gradient $\vec{\nabla}\varphi$ were calculated as functions of the radial distance from the sphere, and plotted in (A) and (B), respectively. The scattering angle is 90° measured from the beam direction. See the text for the other parameter values. The solid lines indicate the exact results, and the symbols are for the numerical results. In the curve labels such as $\{R, n\}$, $R[I]$ stands for the real [imaginary] part, and $n[t]$ for the normal [tangential] component. The plots show that the conventional method gives unreliable results in the vicinity of the surface.

problems that require off-surface field calculation is almost always expensive by nature, requiring the computation at many locations. Thus, the extra task of solving (3.9) adds up only to a fraction of the overall computation, easily compensated by the simplicity and accuracy of the field calculation.

The second remark is that one could eliminate the use of (2.10) by introducing another auxiliary field Ψ in $\overline{V}$ with the alternative boundary condition

$$\nabla_n \Psi = v, \tag{3.10}$$

instead of (3.2). In this case, the additional unknown, i.e., the function Ψ on the boundary ($\equiv p$), must be obtained from the BIE. Once done, the analog of Eq. (3.6) would hold, namely,

$$\begin{aligned} &\chi_P(\vec{\nabla}\varphi)_P + (1-\chi_P)(\vec{\nabla}\Psi)_P \\ &\quad = (\vec{\nabla}\varphi^{(0)})_P + \int_S dS[(\vec{\nabla}G)\times(\vec{n}\times\vec{\nabla}(u-p)) \\ &\qquad - k^2\vec{n}G(u-p)]. \end{aligned} \tag{3.6'}$$

In contrast to (3.6), Eq. (3.6′) represents the normal component continuously. The use of Eqs. (3.5, 3.6, 3.6′) for off-surface calculations would therefore eliminate the use of (2.10) and hence the on-surface point Q from the calculation. The author believes, however, that the method using Eqs. (3.5, 3.7) is superior to this approach because the two auxiliary fields will make the procedure more expensive computationally.

Third, Eqs. (3.5–7) yield ψ and $\vec{\nabla}\psi$ values when the point P is located outside V. Although spurious in the one-phase problem, the analogous results in the two-phase problem are of practical value. (See Sect. 5.)

4. VALIDATION BY NUMERICAL TESTS

The method proposed in Section 3 can be tested numerically, and some of the example calculations are presented in this section. The results of the field computation were reported earlier [3] and are reproduced here for convenience, while the gradient calculations are new results. The test problem is the plane-wave scattering by a spherical body with a radius a, and a boundary condition is imposed so that $v = 0$. The incident field is given by the formula $\varphi^{(0)} = \exp(ikz)$. Accurate solutions for φ and ψ are available by means of partial wave expansions [7], and are referred to as "exact" solutions below. The numerical calculations were performed in two ways for comparison: one by the conventional method based on Eqs. (2.3, 2.4), and the other by the improved method with Eqs. (3.5, 3.7). Other than the different choices of the integral representations, the same numerical algorithms were used throughout the entire calculation to ensure meaningful comparison. For instance, the usual isoparametric, quadrilateral elements were used, and numerical integrals were performed by the Gaussian quadrature. The nodal values of u and w were given by the exact solutions for simplicity, although the standard BEM results can replace them without compromising the accuracy. For actual computations, 64 quadratic elements were used to parametrize the sphere, and the ka value was set to 2.

The near-boundary fields were calculated as functions of lift-off distances from the surface S, and of the polar angle θ

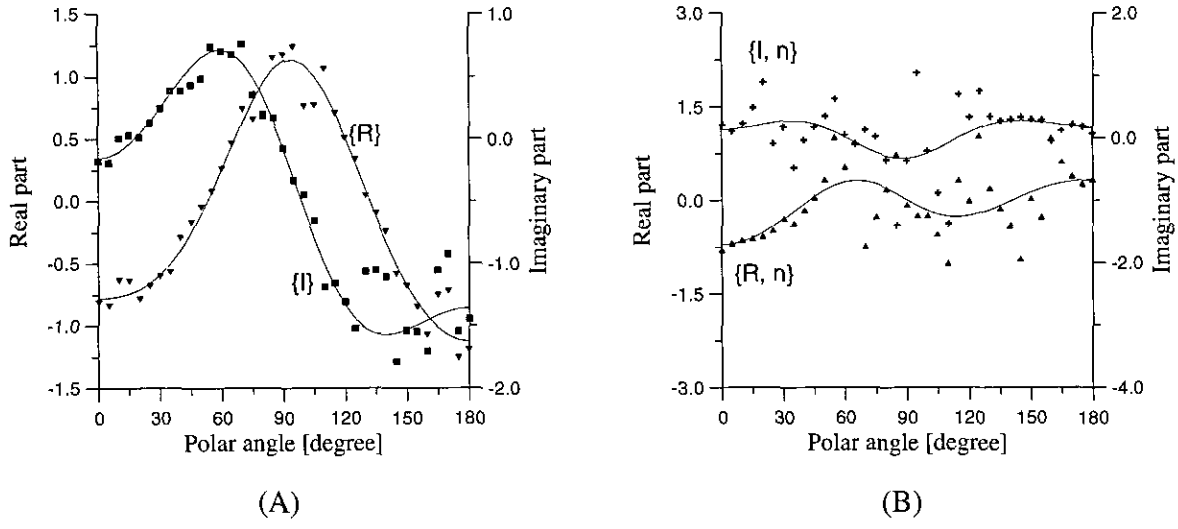

FIG. 2. Plots similar to those in Fig. 1, except that they are plotted against the polar angle θ. (A) is for the field φ and (B) is for the gradient in the normal direction, $\nabla_n\varphi$. The computations were performed slightly outside the sphere, with the lift-off distance equal to 1% of the sphere radius. The $\{R, t\}$ and $\{I, t\}$ results are omitted here. Again, the plots show the instability of the conventional calculation.

measured from the incident direction z. The first set of the results was obtained from Eqs. (2.3, 2.4) by the naive method. A representative subset of the numerical results, accompanied by the exact ones, are plotted in Figs. 1 and 2. The plots exhibit the typical instability discussed in Sect. 2. The second set of the results was derived from Eqs. (3.5, 3.7) by the improved method, and plotted in its entirety in Figs. 3 and 4 that should be compared with Figs. 1 and 2, respectively. The comparisons show clearly that our method is more stable near the boundary surface than the conventional one. Moreover, the stability was achieved without recourse to any special element integration technique. This, therefore, demonstrates the superiority of the representations (3.5, 3.7) over (2.3, 2.4) in expressing fields and derivatives at off-surface locations.

5. IMPROVED FORMULAS FOR MULTIPLE-PHASE PROBLEMS

In Section 3, the scope of our method is restricted to a single-phase problem for a given field φ. It is thus required to introduce an artificial field ψ in the outside region $\bar{V}$ to complement φ. In this section, we will relate the single-phase problem to the multiple-phase problem where such a pair $\{\varphi, \psi\}$ appears more naturally [8]. Without loss of generality, let us consider a two-phase problem where the entire space is separated into V and $\bar{V}$ as before by the surface S. Suppose that there is a field φ_1 in V (or Region "1") and a field φ_2 in $\bar{V}$ (or Region "2"), both satisfying

$$[\nabla^2 + k_a^2]\varphi_a = -J_a, \quad a = 1, 2. \tag{5.1}$$

Let G_a denote Green's functions in V or $\bar{V}$ correspondingly. Also suppose that boundary conditions are imposed across S such that

$$\lambda_1\varphi_1 = \lambda_2\varphi_2 \equiv u, \quad \mu_1(\nabla_n\varphi_1) = \mu_2(\nabla_n\varphi_2) \equiv v, \tag{5.2}$$

where λ_a and μ_a are given constants. Again, the unknown functions u and v on S can be determined accurately by the standard BEM. Notice that Eqs. (5.1, 5.2) are completely analogous to Eqs. (2.1, 2.2, 3.1, 3.2), except that $k_1 \neq k_2$ in general. It hence suffices to list the resulting improved formulas without derivation,

$$\begin{aligned}
&\chi_P(\lambda_1\varphi_1)_P + (1-\chi_P)(\lambda_2\varphi_2)_P \\
&\quad = \lambda_1\varphi_{1P}^{(0)} + \lambda_2\varphi_{2P}^{(0)} + \int_S dS\left[\{-\nabla_n(G_1 - G_2)\}u \right. \\
&\qquad \left. + \left(\frac{\lambda_1}{\mu_1}G_1 - \frac{\lambda_2}{\mu_2}G_2\right)v\right], \qquad (5.3)\\
&\lambda_1\chi_P(\vec{\nabla}\varphi_{1P} - \vec{n}_Q v_Q/\mu_1) + \lambda_2(1-\chi_P)\{\vec{\nabla}\varphi_{2P} - \vec{n}_Q v_Q/\mu_2\} \\
&\quad = \lambda_1\vec{\nabla}\varphi_{1P}^{(0)} + \lambda_2\vec{\nabla}\varphi_{2P}^{(0)} - (\lambda_2/\mu_2)\vec{n}_Q v_Q \\
&\qquad + \int_S dS\left[\{\nabla_n\vec{\nabla}(G_1 - G_2)\}u - \left\{\left(\frac{\lambda_1}{\mu_1}\vec{\nabla}G_1 - \frac{\lambda_2}{\mu_2}\vec{\nabla}G_2\right)v \right.\right. \\
&\qquad \left.\left. - \left(\frac{\lambda_1}{\mu_1} - \frac{\lambda_2}{\mu_2}\right)(\vec{\nabla}G_0)v_Q\right\}\right] \\
&\qquad + \left(\frac{\lambda_1}{\mu_1} - \frac{\lambda_2}{\mu_2}\right)v_Q\int_S dS[(-\vec{\nabla}G_0)(1 - \vec{n}\cdot\vec{n}_Q) \\
&\qquad + (-\vec{\nabla}G_0)\times(\vec{n}\times\vec{n}_Q)], \qquad (5.4)
\end{aligned}$$

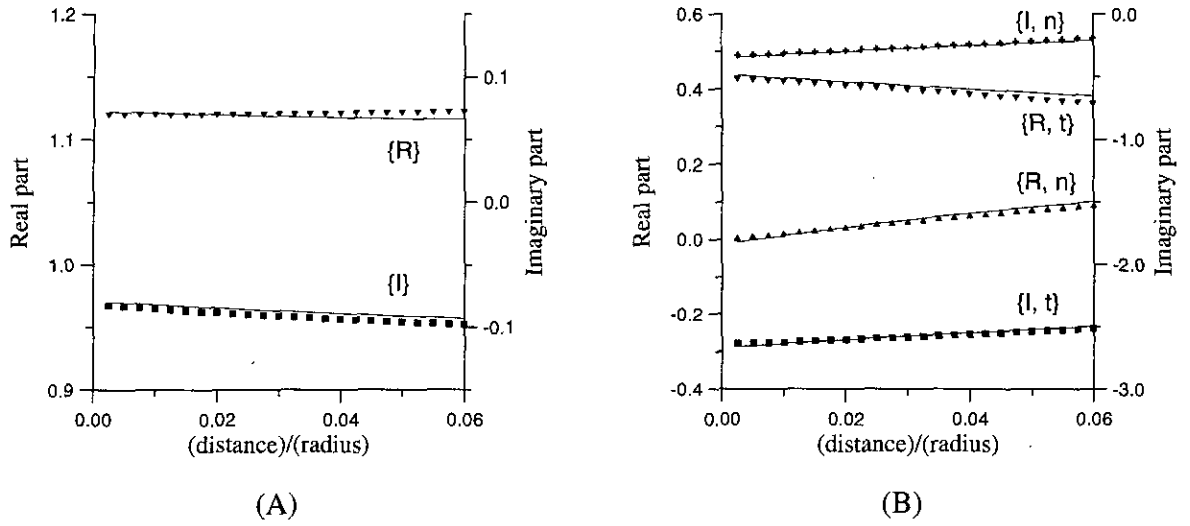

FIG. 3. Plots showing the improved results via Eqs. (3.5, 3.7). The same notation was used as in Fig. 1; for instance, the solid lines are for the exact results and the dots for the numerical ones. The plots clearly demonstrate the improvements on near-boundary field evaluation achieved by the proposed method.

which are analogous to Eqs. (3.5) and (3.7), respectively. Equations (5.3, 5.4) share the desirable features with Eqs. (3.5, 3.7) in representing the fields and the derivatives smoothly. The main differences is that Eqs. (5.3, 5.4) always represent physical quantities, both inside and outside, as remarked at the end of Section 3.

It should be noted that the double-derivative term of (5.4) can be optionally turned into the Maue form that involves tangential u derivatives. Considering that the kernel singularity is equally weak, the above form (5.4) is preferable because the u derivative is absent.

A numerical test of the representations (5.3, 5.4) against exact solutions was carried out in the same manner as found in Section 4 for the single-phase problem. The numerical results are similarly stable and accurate, and hence omitted here.

6. CONCLUDING REMARKS

This paper contends that, when applying the BEM, one should always consider *inside and outside problems in pairs*, irrespective of single-phase or multiple-phase problems. The reason is that, by doing so, one finds the opportunity to cancel

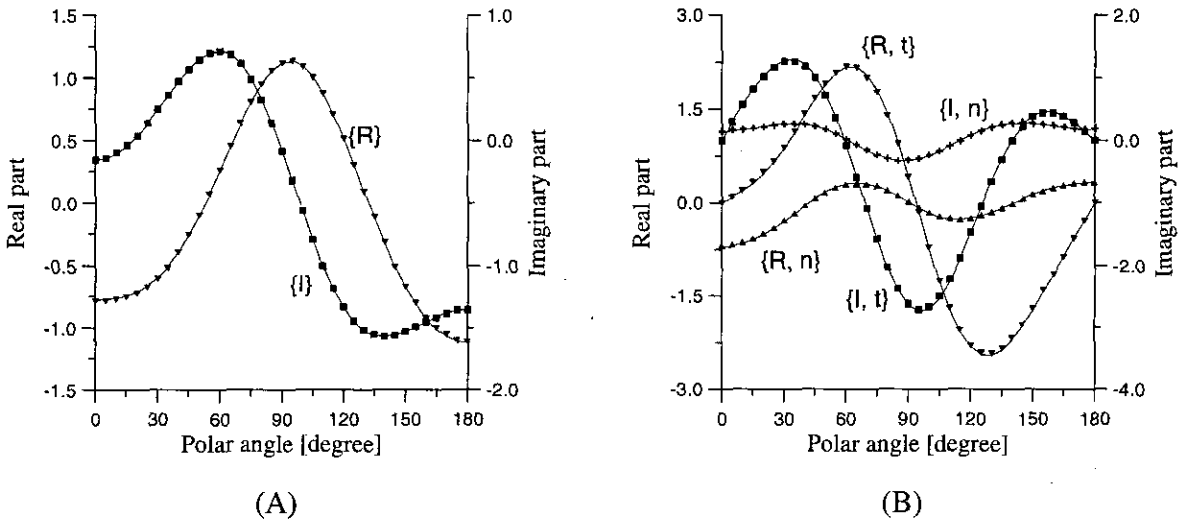

FIG. 4. The improved results vs the polar angle. The plots show improvements over the conventional results of Fig. 2. Here, (B) includes all the components of the gradient $\vec{\nabla}\varphi$. Again, the numerical results (indicated by the dots) coincide with the exact ones (the solid lines) everywhere, including the vicinity of the surface (the lift-off is 1% of the radius).

strong singularities between the basic equations on both sides. Explicitly, the formulation given in Sections 2 and 3 demonstrates that the pair of Green's formulas, (2.3) and (3.3), and the pair of Maue's formulas, (2.4) and (3.4), can cancel singularities between each other, resulting in the improved integral representations (3.5)–(3.7). Equations (3.5)–(3.7) are the main contribution of this paper, forming the foundation of our field evaluation method at off-surface locations. Their validity has been demonstrated by the example computations in Section 4, where it is shown that even a naive element technique can yield smooth and accurate results everywhere including the near-boundary region. The generalization to multiple phase problems is found in Section 5 as Eqs. (5.3, 5.4).

Several remarks are in order. First, other than treating inside and outside problems symmetrically, the present formulation also treats Green's field representation and Maue's gradient representation in a unified fashion. As pointed out in Section 2, this pair results in a set of weakly singular BIEs that has freedom to avoid fictitious frequency problems when necessary. Moreover, it was this systematic, symmetrical treatment of the basic equations that has allowed the discovery of the cancellation mechanism.

Second, this work assumes that the on-surface variables are obtained from the weak version of the BIEs, before off-surface fields are calculated via Eqs. (3.5, 3.7). The merit of this procedure is that the basic formulas are all weakly singular, even before discretization. The choice of the on-surface solution method is not unique, however. A particularly interesting alternative will be the so-called indirect method [6], where the combination $(v - w)$ in Eqs. (3.5, 3.6) is treated as the fundamental unknown and may be determined by the BIEs that follow Eqs. (3.5, 3.6) after the limit is taken. The combination of the indirect BIE method with our off-surface calculation technique may give the most effecient procedure, provided that the indirect BIE can be solved properly.

Third, as explained at the end of Sections 2 and 3, respectively, our off-surface formulas (3.5, 3.7) give the most economical method among the alternatives such as Eqs. (2.11, 2.13) and the two-auxiliary-field approach of Section 3.

Last but not least, we restrict the scope of our discussion to scalar Helmholtz problems throughout this paper. This restriction, however, is only for simplicity, and implies no fundamental limitation as to where the method applies. In fact, the cancellation method applies to a wider class of problems. It is particularly straightforward to generalize the method to electromagnetism because the Stratton–Chu representation [9] is structurally similar to the Maue representation. Generalization to other problems such as elastodynamics and fluid dynamics remains to be carried out in the future.

ACKNOWLEDGMENTS

The author thanks Frank Rizzo for introduction to the problem and for subsequent discussions and encouragement. This work was supported in part by the NSF Industry/University Center for NDE at Iowa State University. This material is also in part based on work performed at the FAA Center for Aviation Systems Reliability operated by Iowa State University and supported by the Federal Aviation Administration under Grant 93-G-029.

REFERENCES

1. G. Green, in *Mathatical Papers of the Late George Green,* edited by N. M. Ferrers (MacMillan, London, 1871), p. 1.
2. A.-W. Maue, *Z. Phys.* **126,** 601 (1949).
3. N. Nakagawa, *Eng. Anal. with Boundary Elements* **13,** 383 (1994).
4. H. Lamb, *Hydrodynamics,* 6th ed. (Dover, New York, 1945).
5. R. F. Harrington, K. Pontoppidan, P. Abrahamsen, and N. C. Albertsen, *Proc. IEE* **116,** 1715 (1969).
6. M. A. Jaswon and G. T. Symm, *Integral Equation Methods in Potential Theory and Elastostatics* (Academic Press, London, 1977), p. 42.
7. P. M. Morse and H. Feshbach, *Methods of Theoretical Physics* (McGraw–Hill, New York, 1953).
8. N. Nakagawa, "Near-Surface Field Evaluation in Two-Phase Helmholtz Problem," in *International Symposium on Boundary Element Methods (IABEM 93), Braunschweig, Germany, August 1993.*
9. J. A. Stratton and L. J. Chu, *Phys. Rev.* **56,** 99 (1939).